Scientific paper

Effect of Fluorinated Ligand on Structural, Electronic and DNA-binding Properties of Copper Paddlewheel Complex: Synthesis, Structure and Properties

Muhammad Iqbal,[1,*] Sqib Ali[2,*] and Muhammad Nawaz Tahir[3]

[1] *Department of Chemistry, Bacha Khan University, Charsadda 24420, KPK, Pakistan*

[2] *Department of Chemistry, Quaid-i-Azam University, Islamabad 45320, Pakistan*

[3] *Department of Physics, University of Sargodha, Sargodha, Pakistan*

* *Corresponding author: E-mail: iqbalmo@yahoo.com, iqbalmo@bkuc.edu.pk (M. Iqbal)*
Tel.: +92 91 6002934; fax: +92 91 6540060.
drsa54@hotmail.com, saqibali@qau.edu.pk (S. Ali).
Tel.: +92 51 90642130; fax: +92 51 90642241.

Received: 17-07-2017

Abstract

This paper presents synthesis, structural description and properties of a binuclear paddlewheel copper(II) carboxylate complex with formula [(py)Cu(μ-L)$_4$Cu(py)], where py = pyridine and L = 4-fluorophenylacetate. Structural characteristics, electronic absorption and DNA-binding properties of the synthesized complex have been compared to those of the non-fluorinated analogues (where F is replaced by H, –CH$_3$ and –OCH$_3$) already reported and the modifications successfully ascribed to fluorine. The complex exhibits typical paddlewheel structure and there are two crystallographically independent molecules in the unit cell. The electronic absorption spectrum of complex is also different and the mode and extent of DNA-binding ability of complex are significantly altered owing to the presence of suitably substituted fluorine. The effect of fluorine is clearly manifested in the modified properties of synthesized complex.

Keywords: *p*-fluorophenylacetate, copper complex, crystal structure, DNA-binding

1. Introduction

The design and synthesis of new functional complexes is the most widely explored area of research in coordination chemistry. Properties of metal complexes arise from metal ion as well as attached ligands. The metal based properties are a function of the type and number of metal ions per molecule. Thus, binuclear complexes have been found to possess enhanced biological, catalytic and magnetic properties compared to the mononuclear analogues.[1–3] Similarly, type and oxidation state of metal ion drastically alter the properties of resulting complex.[4]

The other most important part of a complex are the attached ligands that have a crucial role in steering a complex to its desired properties.[5,6] Ligand not only stabilizes a metal ion in a given oxidation state but also the geometry around it in a coordination complex.[4] Ligands can carry metal ion to its biological target in chemically variable medium of biological systems.[7] The beauty and diversity of synthetic coordination chemistry stems from the variable bonding strength and modes of the ligands having suitable donating sites.[8–10] Moreover, the properties of a complex can be modified *via* changing substituents on the attached ligands.[11,12]

In continuation of our previous work[13–15] we experienced a substantial change in properties of a complex having fluorine substituent instead of hydrogen, methyl and methoxy groups. Modification in structure, absorption spectrum and DNA-binding ability of the fluorous complex were observed compared to other analogues and such alterations have been presented here as a function of fluorine substituent.

2. Experimental

2. 1. Materials and Methods

Anhydrous CuSO$_4$, 4-fluorophenylacetic acid, pyridine, NaHCO$_3$, KCl and sodium salt of salmon sperm

DNA were obtained from Fluka, Switzerland. Solvents like methanol, chloroform and dimethyl sulfoxide were obtained from Merck, Germany, and used as such without drying. Water used was singly distilled. Melting point was obtained in a capillary tube using a Gallenkamp, serial number C040281, U. K, electro-thermal melting point apparatus. FT-IR spectrum was recorded on a Nicolet–6700 FT-IR spectrophotometer, Thermo Scientific, USA, in the range from 4000 to 400 cm^{-1} using attenuated total reflectance (ATR) technique.

2. 2. Single crystal X–ray Crystallographic Study

X-ray single crystal analysis of the complex was performed at 296 K on a Bruker Kappa APEX–II CCD diffractometer using graphite-monochromated Mo-Kα radiation (λ = 0.71073 Å). Crystal structure was solved by direct method followed by final refinement carried on F^2 with full-matrix least-squares using the program SHELXL-97.[16] The H-atoms were included in calculated positions and treated as riding atoms: C–H = 0.93, 0.96 and 0.97 Å for CH, CH_3 and CH_2 H-atoms, respectively, with $U_{iso}(H) = kU_{eq}(C)$, where k = 1.5 for CH_3 and 1.2 for all other H-atoms. One of the ligands in each crystallographically independent molecules is disordered with occupancy ratio of 0.501(10):0.499(10). Benzene rings were treated as regular hexagons with C-atoms having equal anisotropic thermal parameters. Similarly, the substituted fluoro atoms on the phenyl rings were also treated as having equal anisotropic thermal parameters with one another.

2. 3. DNA interaction Study by Cyclic Voltammetry

Voltammetric experiments were performed using an SP–300 potentiostate, serial number 0134, BioLogic Scientific Instruments, France. Measurements were carried out in aqueous DMSO (1:4) solution containing 0.01 M KCl, under an N_2 saturated environment in a conventional three-electrode cell with saturated silver/silver chloride electrode (Ag/AgCl) as reference, a platinum wire as counter and a bare glassy carbon electrode (GCE) with a surface area of 0.196 cm^2 as the working electrode. Prior to experiment, GCE was polished with alumina (Al_2O_3) on a nylon buffing pad followed by washing with acetone and finally with distilled water. Electrochemical measurements were carried out at room temperature (25 ± 0.5 °C).

An appropriate amount of sodium salt of salmon sperm DNA (SSDNA) was dissolved in distilled water and stirred overnight. Nucleotide to protein (N/P) ratio of ~1.9 was obtained from the ratio of absorbance at 260 and 280 nm (A_{260}/A_{280} = 1.9), indicating that SSDNA is sufficiently free from protein.[17] SSDNA concentration was determined *via* absorption spectroscopy using molar absorption coefficient of 6600 M^{-1} cm^{-1} (260 nm) for SSDNA.[18] Voltammograms of 3 mM solution of the complex prepared in aqueous DMSO (1:4) were taken in absence and presence of 10, 20, 30, 40, 50, 60, 70 and 80 μM DNA. Moreover, in order to calculate various redox parameters, cyclic voltamograms were also recorded on 50, 75, 100, 125, 150, 175, 200, 400, 600, 900, 1200 and 1400 mV s^{-1}, before and after adding DNA to solutions of the complex.

2. 4. DNA Interaction Study by Absorption Spectroscopy

Solutions of the complex for UV-Visible spectrophotometric analysis were prepared in aqueous DMSO (1:4) at a concentration of 6 mM. UV absorption titrations were performed by keeping concentration of the complex fixed while varying SSDNA concentration. Equivalent solutions of SSDNA were added to each of complex and reference solutions to eliminate the absorbance of SSDNA itself. Spectra of complex–SSDNA solutions were recorded at room temperature (25 ± 1 °C) using cuvettes of 1 cm path length.

2. 5. Procedure for the Synthesis of Complex

Sodium bicarbonate (0.504 g, 6.00 mmol) was reacted with an equimolar quantity (0.925 g, 6.00 mmol) of 4-fluorophenyl acetic acid at 60 °C in distilled water. After complete neutralization of acid with base, aqueous solution of copper sulphate (0.478 g, 3.00 mmol) was added drop wise. The reaction mixture was stirred for 3 h at 60 °C as depicted in Scheme 1. This was followed by the addition of methanolic solution of pyridine (0.24 mL, 3.0 mmol) with continued stirring for further 3 h under same reaction conditions. The final product was filtered, washed thoroughly with distilled water and air dried. The dried solid was recrystallized from a mixture of chloroform and methanol (1:1).

Light blue crystals; m.p. 182–183 °C; Yield (70%). FT-IR (cm^{-1}): $\nu(OCO)_{asym}$ = 1650, $\nu(OCO)_{sym}$ = 1442 ($\Delta\nu$ = 208), νCH_2 = 2920, ν(Ar–H) = 3031, ν(Ar–F) = 1162, νAr(C=C) = 1586 and 1438, ν(Cu–O) = 422, ν(Cu–N) = 475.

3. Results and Discussion

3. 1. FT-IR Data

FT-IR spectrum of the complex contained all characteristic bands. The bonding mode of carboxylate moiety was indicated by its characteristic intense bands at 1650 and 1442 cm^{-1} corresponding to asymmetric and symmetric OCO stretching vibrations, respectively. This was supported by the appearance of a Cu–O absorption band at 422 cm^{-1} which indicated coordination of the carboxylate ligand through oxygen. Value of $\Delta\nu = \{\nu_{asym}(OCO) -$

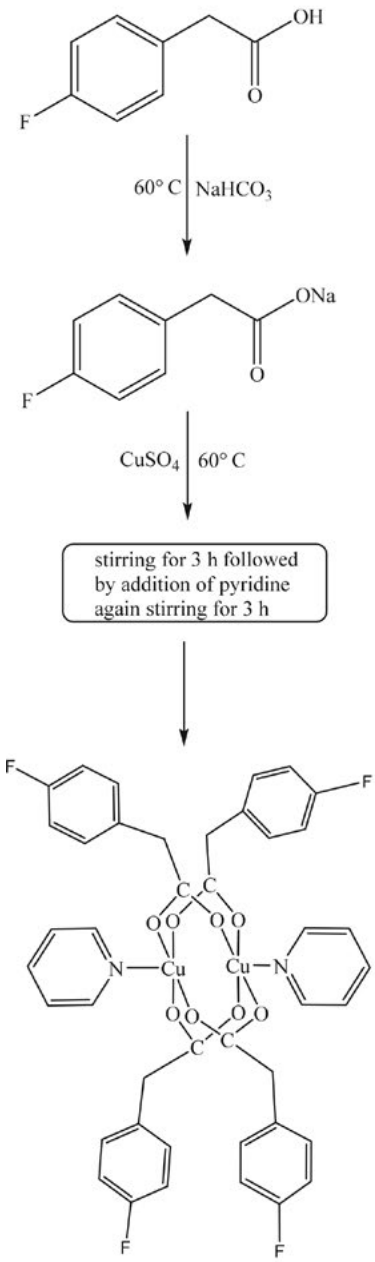

Scheme 1. Synthetic procedure for complex

ν_{sym}(OCO)} calculated for complex was 208 cm^{-1} showing bonding modes of carboxylate moiety to copper(II) ion typical of brigding bidentate fashion.[19] In addition, the appearance of C=N stretching band of complex at a frequency of 1592 cm^{-1} instead of its normally observed characteristic region (1610–1625 cm^{-1})[20,21] indicated the involvement of nitrogen atom of pyridine in bonding with copper(II) ion.[22] This was further supported by the appearance of a new medium intensity band at 475 cm^{-1} attributable to a Cu–N vibration.[23] Aromatic C=C and C–H stretching vibrations were observed at 1586 and 1438 and 3031 cm^{-1}, respectively. Methylene C–H stretching frequency of complex was observed at 2920 cm^{-1}, supported by the presence of bands at 692 and 1398 cm^{-1} corresponding to its rocking and bending deformations, respectively.

3. 2. Crystal Structure Description

Ortep diagram of complex with atom numbering scheme is shown in Fig. 1 and crystal refinement parameters and important bond lengths and angles are given in Tables 1 and 2. Complex crystallizes in triclinic system with space group *P*–1 having two crystallographically independent molecules in the unit cell as shown in Fig. 2. Complex displays the classical paddlewheel structure having four carboxylate ligands bonded in a syn–syn configuration, bridging the two copper(II) ions. The coordination environment around each copper ion is {$CuNO_4$} where four oxygen atoms of carboxylate ligands occupy the square base while a pyridine molecule occupies the axial coordination site resulting in square pyramidal coordination geometry for each Cu(II) ion. The Cu···Cu and average Cu–O distances are 2.6411(8) and 1.9585(4) Å, respectively, which are close to those observed for structurally related dimer of Cu(II) ions with trifluoroacetate and phenylacetate ligands already reported [$Cu_2(CF_3CO_2)_4(CH_3CN)_2$] (where Cu···Cu = 2.766(1) and Cu–O = 1.969(5) Å).[24–26] Cu–N distance (2.174(4) Å) is comparable to those found for apical N-donor acetonitrile ligand (2.114(2) Å)[25] but longer than those found for imidazole N-donor ligand (1.9815(15) Å) in mononuclear octahedral carboxylate complex.[27] This is attributed to the elongation of apical Cu–ligand bond distance as a consequence of repulsion exerted by the doubly occupied d_{z2}-orbital along this axis.[28] However, the basic strength of the N-donor ligand also determines the Cu–N bond length.[29] The trans angles

Table 1. Structure refinement parameters of the complex

Chemical formula	**$C_{42}H_{34}F_4Cu_2N_2O_8$**
FW (g mol^{-1})	897.79
Temperature (K)	296(2)
Crystal system	Triclinic
Space group	P –1
a (Å)	12.0582(3)
b (Å)	12.9571(4)
c (Å)	14.6191(4)
α (°)	78.873(2)
β (°)	74.229(3)
γ (°)	69.542(2)
V (Å^3)	2047.26(11)
Z	2
ρ_{calc} (g cm^{-3})	1.456
Absorption coeff. (mm^{-1})	1.111
F(000)	916
Reflections collected	30120
Independent reflections	7330
Data/restraints/parameters	7330 / 8 / 530
Goodness-of-fit on F^2	0.988
$R[F^2 > 2\,\sigma(F^2)]$, $wR(F^2)$	0.0482, 0.110

(O–Cu–O) of the square base, consisting of four O atoms in complex are 167.76(15) and 168.15(12)°. Moreover, all the O–Cu···Cu bond angles in complex range from 82.5(1) to 85.4(1)° while the O–Cu–N bond angles are in the range 89.19(16)–100.03(16)°. All these angle ranges are typical of paddlewheel type complexes. The molecule is centrosymmetric with center of inversion at midpoint between two copper ions.

Table 2. Selected Bond lengths and angles of complex

Distances, Å	
Cu1–O1	1.958(4)
Cu1–O2	1.952(4)
Cu1–O3	1.961(4)
Cu1–O4	1.953(4)
Cu1–N1	2.174(4)
Cu1–Cu1	2.6411(8)
Angles,°	
O4–Cu1–O1	87.90(16)
O2–Cu1–O3	89.48(16)
O1–Cu1–O2	97.04(16)
O4–Cu1–O3	90.92(16)
O1–Cu1–O3	167.76(15)
O4–Cu1–O2	168.15(12)
O4–Cu1–N1	100.03(16)
O1–Cu1–N1	92.15(13)
O2–Cu1–N1	89.19(16)
O3–Cu1–N1	94.78(16)
O4–Cu1–Cu1	82.5(1)
O1–Cu1–Cu1	84.7(1)
O2–Cu1–Cu1	83.5(1)
O3–Cu1–Cu1	85.4(1)
N1–Cu1–Cu1	174.4(1)

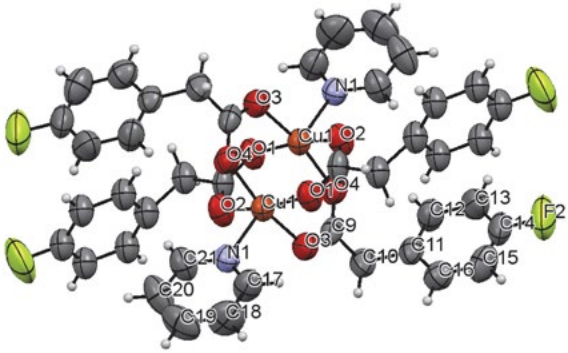

Fig. 1. Structure of the complex tetrakis(4-fluorophenylacetato-μ-*O*,*O*')bis(pyridine-*N*)dicopper(II) with numbering scheme.

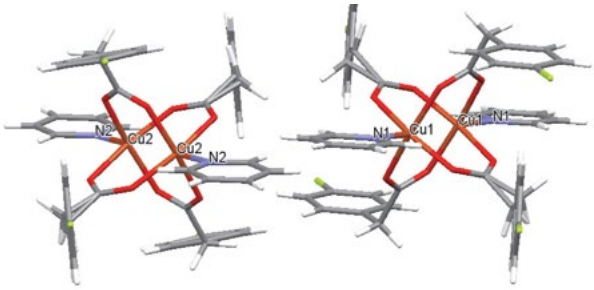

Fig. 2. Two crystallographically independent molecules in the unit cell.

Supramolecular structure: Crystal packing of complex is shown in Fig. 3, which is quite different from that of 4-chlorophenylacetate complex with copper,[15] although one might think that there is mere replacement of F for Cl. It may be due to the presence of two crystallographically independent molecules in the unit cell of the former complex. Similarly, C–H···O type interactions are found between hydrogen atoms of C10–H10B and O8 and C31–H31B and O3.

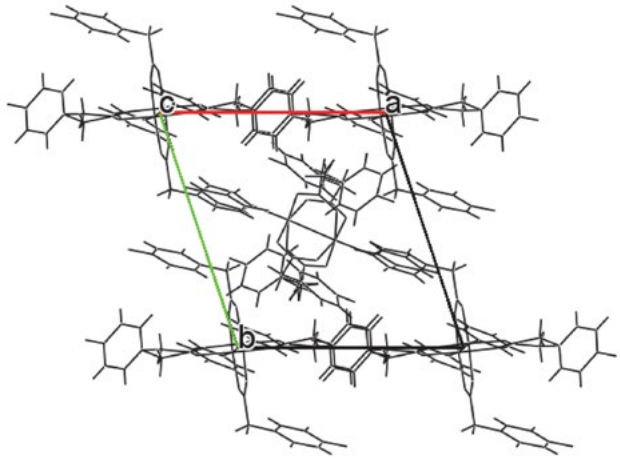

Fig. 3. Packing diagram of the complex along *c*-axis.

3. 3. Cyclic Voltammetry

Electrochemical study of the complex shows an anodic peak at 0.175 V corresponding to Cu(I)/Cu(II) process and a cathodic peak at –0.20 V corresponding to Cu(II)/Cu(I) reduction.[2,30] The higher value of peak separation precludes the possibility of reversibility of two redox processes as shown in Fig. 4A.

DNA binding study through cyclic voltammetry

Cyclic voltammetry was employed to explore DNA binding ability of complex at various scan rates. The shift in peak potential was used to decide about the mode of DNA binding activity of complex. A negative shift in peak potential i.e., to less positive region (or to more negative region in case of reduction signal) on addition of DNA indicates electrostatic mode of interaction with complex,[31,32] while a positive shift in potential i.e., to more positive region (or to less negative region in case of reduction signal) exhibits an intercalative mode. However, pure electrostatic or intercalative modes of interaction are seldom encountered and more often a mixed behavior is usually observed.

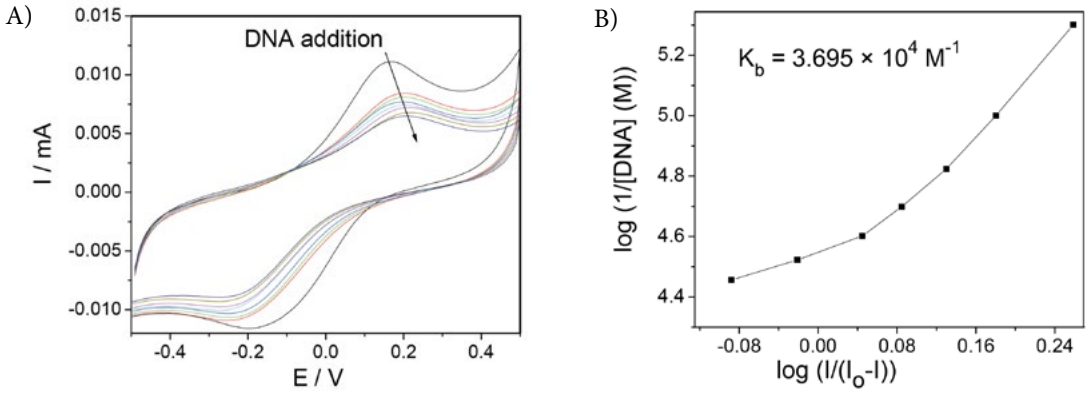

Fig. 4. A: voltamograms of complex at scan rate 100 mV/s in absence and presence of DNA showing a shift in peak potential towards more positive values. **B**: plot for calculation of binding constant K_b.

Anodic peak of synthesized complex experienced shift to more positive region (or to less negative region in the case of reduction peaks) with addition of DNA. On successive DNA addition there is further shifting of peak potential to more positive potential region as shown in Fig. 4A. This type of binding with DNA is termed as intercalative mode. The predominant intercalative ability of the complex is ascribed to the presence of planar aromatic rings. However, since fluoro groups are more efficient electrostatic binders, there must be a significant contribution of electrostatic interaction to the binding of complex along with intercalation between DNA base pairs.

In addition to peak shift, peak current experienced a diminution on the addition of DNA to complex solution. On the basis of decrease in peak current of the unbound complex by addition of different concentrations (10 to 80 μM) of SSDNA, the binding constant was calculated. The plot of log 1/[DNA] *vs.* log $I/(I_o - I)$ gave rise to a straight line (Fig. 4B), whose intercept was used to calculate the binding constant using an already reported procedure.[33] The value of K_b calculated for complex was $3.695 \times 10^4\ M^{-1}$ which is higher than those of the non-fluorinated structural analogues where F is substituted by H, $-CH_3$ and $-OCH_3$,[13–15] having K_b values 0.033×10^4, 1.44×10^4 and $1.007 \times 10^4\ M^{-1}$, respectively. Since the rest of structural parameters are the same, the higher value of K_b must be due to the presence of *para*-fluoro groups, enhancing interaction of complex with DNA. It can be inferred that there is electrostatic interaction of complex owing to the electronegative F atom along with intercalation of aromatic rings. This leads to facile formation of complex-DNA adduct leading to relatively higher K_b value.

The DNA binding ability of the complex was also confirmed by calculating the diffusion coefficient of complex before and after DNA addition. This was accomplished by measuring voltammograms at different scan rates before and after DNA addition and putting the relevant parameters in the Randles-Sevcik equation.[34]

The slope values for D_o calculation were obtained making use of the respective i_p *vs.* $v^{1/2}$ plots for oxidation process employing Bard and Faulkner relation.[35]

Values of D_o thus calculated for complex before and after DNA addition were 7.912×10^{-8} and 0.305×10^{-8} cm^2s^{-1}. The lower value of diffusion coefficient of DNA-bound complex compared to that of the unbound complex shows a reduction in the mobility of the former.[36,37] The reduction in mobility of complex with DNA addition shows adduct formation between the two having hampered mobility in solution.

3. 4. Absorption Spectroscopy

The complex exhibited a broad absorption band (shown in Fig. 5A) with λ_{max} = 737 nm corresponding to *d-d* transition of Cu^{2+} and has been found typical of square pyramidal copper(II) geometry in solution.[38–40] This shows the relative stability of paddlewheel structure and that square pyramidal structure is retained in solution. The band in *d-d* region is expected to be sensitive to the nature (basicity and bond length) of attached apical and basal ligands. As the bond length of attached ligands increases, the band is shifted to shorter wavelength (higher energy) region.[41] The same has been observed here where the non-fluoro analogues (where F is replaced by H,[13] CH_3,[14] OCH_3[15]) give rise to bands at 720 nm with Cu–N_{av} distance of 2.158(2) Å compared to 2.174(4) Å of the synthesized fluoro-complex. Using Beer-Lambert's Law, ε value has been calculated to be 141 ($L\ mol^{-1}\ cm^{-1}$) for complex.

DNA study through absorption spectroscopy

The variation in λ_{max} of complex on addition of DNA can be used to measure the ability of complex to bind with DNA. A blue shift in λ_{max} indicates electrostatic while red shift indicates intercalative mode of interaction with DNA.[42,43] Shift in λ_{max} is usually accompanied with a pronounced decrease in absorbance which can be used to calculate the extent of interaction i.e., binding constant K_b. On successive addition of 10–70 μM DNA to complex

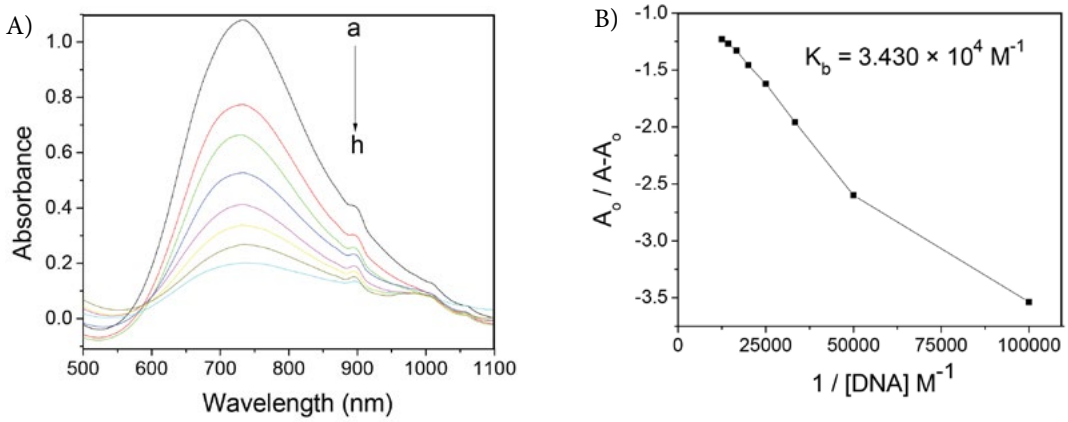

Fig. 5. A, reduction in absorbance of pure complex with addition of DNA. **B**, plot for calculation of binding constant K_b.

solution, there was extensive reduction in absorbance of complex along with a small red shift as shown in Fig. 5A. Using the famous Benesi-Hildebrand equation,[44] the binding constant was calculated from slope to intercept ratio of the plot of $A_o/A - A_o$ *vs*. 1/[DNA] as shown in Fig. 5B. Value of K_b was found out to be $3.430 \times 10^4\ M^{-1}$ which is in good agreement with K_b value obtained through cyclic voltammetry. The binding mode of complex has been found to be mixed type where intercalation is accompanied by electrostatic groove binding mode as well. The later binding mode may be due to the presence of polar fluoro group which enhances electrostatic interaction with DNA. Thus, the properties of complex have been modified substantially on changing the substituent on attached ligand.

4. Conclusion

A new copper(II) complex has been synthesized which represents new addition to the existing database on paddlewheel type complexes. Its structural, electronic absorption and DNA-binding properties have been compared to those of the non-fluorinated analogues. The peak position in absorption spectrum of complex is shifted in accordance to the altered basic strength of fluorophenylacetate ligand. Electrostatic contribution is included in DNA-binding mode of complex and the extent of DNA-binding is enhanced three times owing to the presence of fluorine in complex. The effect of fluorine is clearly manifested in the modified properties of synthesized complex.

Supplementary data: Crystallographic data for the structure reported in this paper has been deposited with the Cambridge Crystallographic Data Centre, CCDC # 934064. Copies of this may be obtained free of charge from The Director, CCDC, 12, Union Road Cambridge CB2 1EZ [Fax: +44 (1223)336 033] or e.mail: deposit@ccdc.cam.ac.uk.

5. References

1. C. Lipinski, A. Hopkins, *Nature* **2004**, *432*, 855-861. **DOI:**10.1038/nature03193
2. N. V. Kulkarni, A. Kamath, S. Budagumpi, V. K. Revankar, *J. Mol. Struct*. **2011**, *1006* 580–588. **DOI:**10.1016/j.molstruc.2011.10.008
3. A. Prisecaru, M. Devereux, N. Barron, M. McCann, J. Colleran, A. Casey, V. McKee, A. Kellett, *Chem. Commun*. **2012**, *48*, 6906–6908. **DOI:**10.1039/c2cc31023f
4. T. Storr, P. Verma, R. C. Pratt, E. C. Wasinger, Y. Shimazaki, T. D. P. Stack, *J. Am. Chem. Soc*. **2008**, *130*, 15448–15459. **DOI:**10.1021/ja804339m
5. E. V. Nosova, T. N. Moshkina, G. N. Lipunova, I. V. Baklanova, P. A. Slepukhin, V. N. Charushin, *J. Fluorine Chem*. **2015**, *175*, 145–151. **DOI:**10.1016/j.jfluchem.2015.04.010
6. J. Zhu, C. Ni, B. Gao, J. Hu, *J. Fluorine Chem*. **2015**, *171*, 139–147. **DOI:**10.1016/j.jfluchem.2014.08.011
7. P. Ruiz-Sanchez, C. Konig, S. Ferrari, R. Alberto, *J. Biol. Inorg. Chem*. **2011**, *16*, 33–44. **DOI:**10.1007/s00775-010-0697-z
8. D. Barut, N. Korkmaz, S. T. Astley, M. Aygün, *Acta Chim. Slov*. **2015**, *62*, 88–94. **DOI:**10.17344/acsi.2014.734
9. X.-Z. Zhang, Y. Gu, Y. Li, A. Liu, F. Liu, Z. You, H.-L. Zhu, *Acta Chim. Slov*. **2016**, *63*, 721–725. **DOI:**10.17344/acsi.2016.2421
10. A. Mushtaq, S. Ali, M. N. Tahir, H. Ismail, B. Mirza, M. Saadiq, M. A. Haleem, M. Iqbal, *Acta Chim. Slov*. **2017**, *64*, 397–408. **DOI:**10.17344/acsi.2017.3250
11. V. T. Kasumov, F. Suzergoz, E. Sahin, O. Celik, M. Aslanoglu, *J. Fluorine Chem*. **2014**, *162*, 78–89. **DOI:**10.1016/j.jfluchem.2014.03.011
12. T. M. Jeitner, E. Kristoferson, J. A. Azcona, J. T. Pinto, C. Stalnecker, J. W. Erickson, H. F. Kung, J. Li, K. Ploessl, A. J. L. Cooper, *J. Fluorine Chem*. **2016**, *192*, 58–67. **DOI:**10.1016/j.jfluchem.2016.10.008
13. M. Iqbal, S. Ali, Z.-U. Rehman, N. Muhammad, M. Sohail, V. Pandarinathan, *J. Coord. Chem*. **2014**, *67*, 1731–1745. **DOI:**10.1080/00958972.2014.926337
14. M. Iqbal, S. Ali, N. Muhammad, M. Sohail, *Polyhedron* **2013**, *57*, 83–93. **DOI:**10.1016/j.poly.2013.04.020
15. M. Iqbal, I. Ahmad, S. Ali, N. Muhammad, S. Ahmed, M.

Sohail, *Polyhedron* **2013**, *50*, 524–531. **DOI:**10.1016/j.poly.2012.11.037
16. G. M. Sheldrick, *Acta Cryst*. **2008**, *A 64*, 112–122.
17. S. Dey, S. Sarkar, H. Paul, E. Zangrando, P. Chattopadhyay, *Polyhedron* **2010**, *29*, 1583–1587. **DOI:**10.1016/j.poly.2010.01.022
18. C. V. Sastri, D. Eswaramoorthy, L. Giribabu, B. G. Maiya, *J. Inorg. Biochem*. **2003**, *94*, 138–145. **DOI:**10.1016/S0162-0134(02)00622-0
19. S. Leconte, R. Ruzziconi, *J. Fluorine Chem*. **2002**,*117*, 167–172. **DOI:**10.1016/S0022-1139(02)00161-6
20. K. V. Shuvaev, S. Sproules, J. M. Rautiainen, E. J. L. McInnes, D. Collison, C. E. Anson, A. K. Powell, *Dalton Trans*. **2013**, *42*, 2371–2381. **DOI:**10.1039/C2DT31946B
21. C. Jayabalakrishnan, K. Natarajan, *Transit. Met. Chem*. **2002**, *27*, 75–79. **DOI:**10.1023/A:1013437203247
22. Z. H. Abd El-Wahab, M. M. Mashaly, A. A. Salman, B. A. El-Shetary, A. A. Faheim, *Spectrochim. Acta A* **2004**, *60*, 2861–2873. **DOI:**10.1016/j.saa.2004.01.021
23. M. Shakir, N. Begum, S. Parveen, P. Chingsubam, S. Tabassum, *Synth. React. Inorg. Met. Org. Chem*. **2004**, *34*, 1135–1148. **DOI:**10.1081/SIM-120039262
24. A. Motreff, R. C. da Costa, H. Allouchi, M. Duttine, C. Mathoniere, C. Duboc, J. M. Vincent, *J. Fluorine Chem*. **2012**, *134*, 49–55. **DOI:**10.1016/j.jfluchem.2011.03.002
25. M. Iqbal, M. Sirajuddin, S. Ali, M. Sohail, M. N. Tahir, *Inorg. Chim. Acta* **2016**, *440*, 129–138. **DOI:**10.1016/j.ica.2015.10.042
26. B. Shen, P.-F. Shi, Y.-L. Hou, F.-F. Wan, D.-L. Gao, B. Zhao, *Dalton Trans*. **2013**, *42*, 3455–3463. **DOI:**10.1039/C2DT32515B
27. M. A. Agotegaray, M. Dennehy, M. A. Boeris, M. A. Grela, R. A. Burrow, O. V. Quinzani, *Polyhedron* **2012**, *34*, 74–83. **DOI:**10.1016/j.poly.2011.12.005
28. M. A. Halcrow, *Chem. Soc. Rev*. **2013**, *42*, 1784–1795. **DOI:**10.1039/C2CS35253B
29. A. S. Potapov, G. A. Domina, T. V. Petrenko, A. I. Khlebnikov, *Polyhedron* **2012**, *33*, 150–157. **DOI:**10.1016/j.poly.2011.11.039
30. C. Di Nicola, F. Garau, Y. Y. Karabach, L. M. D. R. S. Martins, M. Monari, L. Pandolfo, C. Pettinari, A. J. L. Pombeiro, *Eur. J. Inorg. Chem*. **2009**, 666–676. **DOI:**10.1002/ejic.200800842
31. M. T. Carter, M. Rodriguez, A. J. Bard, *J. Am. Chem. Soc*. **1989**, *111*, 8901–8911. **DOI:**10.1021/ja00206a020
32. M. S. Mohamed, A. A. Shoukry, A. G. Ali, *Spectrochim. Acta Part A* **2012**, *86*, 562–570. **DOI:**10.1016/j.saa.2011.11.015
33. Q. Feng, N. Q. Li, Y. Y. Jiang, *Anal. Chim. Acta* **1997**, *344*, 97–104. **DOI:**10.1016/S0003-2670(97)00008-1
34. J. Wang, Analytical Electrochemistry, 1st ed., VCH Publishers, 1994, pp. 165–166.
35. A. J. Bard and L. R. Faulkner, Electrochemical Methods, Fundamentals and Applications, 2nd ed., Wiley, New York, 2004, p-236.
36. M. Chauhan, K. Banerjee, F. Arjmand, *Inorg. Chem*. **2007**, *46*, 3072–3082. **DOI:**10.1021/ic061753a
37. G.-Y. Li, K.-J. Du, J.-Q. Wang, J.-W. Liang, J.-F. Kou, X.-J. Hou, L.-N. Ji, H. Chao, *J. Inorg. Biochem*. **2013**, *119*, 43–53. **DOI:**10.1016/j.jinorgbio.2012.09.019
38. S. Majumder, M. Fleck, C. R. Lucas, S. Mohanta, *J. Mol. Struct*. **2012**, *1020*, 127–133. **DOI:**10.1016/j.molstruc.2012.04.003
39. S. S. Massoud, F. R. Louka, Y. K. Obaid, R. Vicente, J. Ribas, R. C. Fischer, F. A. Mautner, *Dalton Trans*. **2013**, *42*, 3968–3978. **DOI:**10.1039/c2dt32540c
40. A. Domínguez-Martín, D. Choquesillo-Lazarte, J. A. Dobado, I. Vidal, L. Lezama, J. M. González-Pérez, A. Castiñeiras, J. Niclós-Gutiérrez, *Dalton Trans*. **2013**, *42*, 6119–6130. **DOI:**10.1039/c2dt32191b
41. A. Theodorou, M. A. Demertzis, D. Kovala-Demertzi, E. E. Lioliou, A. A. Pantazaki, D. A. Kyriakidis, *BioMetals* **1999**, *12*, 167–172. **DOI:**10.1023/A:1009246122577
42. L. Jia, J. Shi, Z.-H. Sun, F.-F. Li, Y. Wang, W.-N. Wu, Q. Wang, *Inorg. Chim. Acta* **2012**, *391*, 121–129. **DOI:**10.1016/j.ica.2012.05.014
43. X. Li, Y.-T. Li, Z.-Y. Wu, Y.-J. Zheng, C.-W. Yan, *Inorg. Chim. Acta* **2012**, *385*, 150–157. **DOI:**10.1016/j.ica.2012.01.047
44. M. Y. Ni, Y. Wang, H. L. Li, *Pol. J .Chem*. **1997**, *71*, 816–822.

Povzetek

V prispevku predstavljamo sintezo, strukturo in lastnosti dvojedrnega bakrovega(II) karboksilato kompleksa s formulo $[(py)Cu(\mu\text{-}L)_4Cu(py)]$, kjer je py = piridin in L = 4-fluorofenilacetat. Strukturne značilnosti in elektronsko absorpcijo sintetiziranega kompleksa ter vezavo na DNA smo primerjali z že objavljenimi nefluoriranimi analogi (kjer so na mestu F atoma vezane H, $-CH_3$ in $-OCH_3$ skupine) ter modifikacije pripisali prisotnemu fluorovemu atomu. Kompleks ima tipično strukturo vodnega kolesa. V asimetrični enoti sta prisotni dve kristalografsko neodvisni molekuli. Elektronski absorpcijski spekter kompleksa se razlikuje od nefluoriranih analogov, opazna je tudi razlika v načinu in jakosti vezave na DNA zaradi prisotnega fluoro substituenta. Vpliv fluorovega atoma je razviden na podlagi spremenjenih lastnosti sintetiziranega kompleksa.